AGU PUBLICATIONS

Water Resources Research

RESEARCH ARTICLE
10.1002/2014WR016433

Companion to *Queloz et al.* [2015], doi:10.1002/2014WR016508.

Key Points:
- Experimental storage and sampling of water and solutes
- Degradation and uptake of fluorobenzoate tracers in unsaturated conditions
- Measures of solute uptake by vegetation are essential to flow kinematics

Supporting Information:
- Supporting Information S1
- Data Set S1
- Data Set S2
- Data Set S3
- Data Set S4
- Data Set S5

Correspondence to:
A. Rinaldo,
andrea.rinaldo@epfl.ch

Citation:
Queloz, P., E. Bertuzzo, L. Carraro, G. Botter, F. Miglietta, P. S. C. Rao, and A. Rinaldo (2015), Transport of fluorobenzoate tracers in a vegetated hydrologic control volume: 1. Experimental results, *Water Resour. Res.*, *51*, 2773–2792, doi:10.1002/2014WR016433.

Received 7 OCT 2014
Accepted 19 MAR 2015
Accepted article online 24 MAR 2015
Published online 26 APR 2015

Transport of fluorobenzoate tracers in a vegetated hydrologic control volume: 1. Experimental results

Pierre Queloz[1], Enrico Bertuzzo[1], Luca Carraro[1,2], Gianluca Botter[2], Franco Miglietta[3], P. S. C. Rao[4], and Andrea Rinaldo[1,2]

[1]Laboratory of Ecohydrology, Ecole Polytechnique Fédérale de Lausanne, Lausanne, Switzerland, [2]DICEA, University of Padova, Padova, Italy, [3]Istituto di Biometeorologia IBIMET-CNR, Firenze, Italy, [4]School of Civil Engineering, Purdue University, West Lafayette, *Indiana, USA*

Abstract This paper reports about the experimental evidence collected on the transport of five fluorobenzoate tracers injected under controlled conditions in a vegetated hydrologic volume, a large lysimeter (fitted with load cells, sampling ports, and an underground chamber) where two willows prompting large evapotranspiration fluxes had been grown. The relevance of the study lies in the direct and indirect measures of the ways in which hydrologic fluxes, in this case, evapotranspiration from the upper surface and discharge from the bottom drainage, sample water and solutes in storage at different times under variable hydrologic forcings. Methods involve the accurate control of hydrologic inputs and outputs and a large number of suitable chemical analyses of water samples in discharge waters. Mass extraction from biomass has also been performed ex post. The results of the 2 year long experiment established that our initial premises on the tracers' behavior, known to be sorption-free under saturated conditions which we verified in column leaching tests, were unsuitable as large differences in mass recovery appeared. Issues on reactivity thus arose and were addressed in the paper, in this case attributed to microbial degradation and solute plant uptake. Our results suggest previously unknown features of fluorobenzoate compounds as hydrologic tracers, potentially interesting for catchment studies owing to their suitability for distinguishable multiple injections, and an outlook on direct experimental closures of mass balance in hydrologic transport volumes involving fluxes that are likely to sample differently stored water and solutes.

1. Introduction

The intertwined dynamics of catchment water storage, connectivity of flow pathways, and heterogeneous reactions are key to our understanding of basin-scale transport in the hydrologic response [e.g., *Beven*, 2012]. One outstanding challenge to a general theory, subsumed by the so-called old-water paradox [*McDonnell et al*., 2010], concerns the stationarity of the response of hydrologic transport volumes to erratic and nonpoint source inputs [e.g., *McDonnell and Beven*, 2014]. Stationarity, or the lack of it thereof, centers attention on how catchments store and release water and solutes [*Botter et al*., 2010, 2011; *Rinaldo et al*., 2011; *van der Velde et al*., 2012; *Hrachowitz et al*., 2013; *Benettin et al*., 2013; *Bertuzzo et al*., 2013; *Benettin et al*., 2014; *Harman*, 2015]. Specifically, the mass response to a specific rainfall event is now acknowledged to be composed by water labeled by different residence times in the transport volume since injection (i.e., the "ages"), not necessarily (and almost inevitably not) generated by the latest event [e.g., *Stewart and McDonnell*, 1991; *Divine and McDonnell*, 2005; *McGuire and McDonnell*, 2006; *McGuire et al*., 2007]. The mixture of different ages of residence within the catchment results from transport and by differential sampling operated by outflows among water parcels in storage. When and how discharge samples within complex catchment control volumes is thus a fundamental open issue.

In soil profiles, matrix heterogeneities and lack of stationarity of the processes dominate the ephemeral triggering of preferential flow paths in unsaturated conditions, and thus the issue of determining the distributions of residence times of water in storage [e.g., *Flury et al*., 1994]. Chemically variable, basin-scale storage recharge integrates instead the stochasticity of climatic forcings, the sources of water and solutes, flow path heterogeneities, and fluctuating evapotranspiration form diverse assemblages of vegetation [*Stewart and McDonnell*, 1991; *Kirchner et al*., 2010; *McGuire and McDonnell*, 2006; *McDonnell et al*., 2010], with implications on large-scale transport. In fact, the ages in storage are a measure of the contact time between fixed and

mobile phases driving mass exchange processes and biogeochemical reactions [*Rinaldo and Marani*, 1987; *Rinaldo et al*., 1989; *Stewart and McDonnell*, 1991]. Age distributions are thus effective descriptors of biogeochemical function of a catchment including its export of anthropogenic inputs [*Brusseau et al*., 1989; *Flury*, 1996; *Wolock et al*., 1997; *McGuire and McDonnell*, 2006; *Hrachowitz et al*., 2010a, 2010b; *Bertuzzo et al*., 2013].

Direct experimental measure of residence time distributions within a hydrological system proves a difficult task. It would, in principle, require the tagging of every water particle to record the time elapsed from its injection to the exit from the system, measuring all outfluxes at frequencies comparable with the relevant time scale of hydrologic fluctuations and extending the measure until full delivery (typically, months to years). Natural or artificial tracers have been used to that end. One method consists of tracking water molecules by using the water natural stable isotopes oxygen-18 (^{18}O) and deuterium (^{2}H). By measuring isotopic fluctuations in both input and output water, one can infer the age structure of the water within a catchment for as long a record as the input characterization allows [e.g., *Lindstrom and Rodhe*, 1986; *Rodhe et al*., 1996; *Maloszewski et al*., 1992; *Kendall and Caldwell*, 1998; *Simic and Destouni*, 1999; *Kirchner et al*., 2010]. Another approach consists of artificially injecting into the hydrologic system nonnative soluble substances as a tool for tracking water molecules. This method has the advantage that the input can be noncontinuous and controlled and that several different tracers can be injected sequentially. When sampling outfluxes, the detection of a specific tracer would then be a direct measure of the travel time distribution (the residence times sampled at the exit) if injection into the system were unique and instantaneous. However, perfect tracers and high-frequency tagging for months or years do not exist in practice, because of the analytical burden implied and because most of the soluble compounds used as hydrologic tracers to date can undergo selective plant uptake, biogeochemical and/or microbial degradation, and retardation processes [e.g., *Käss*, 1998; *Flury*, 2003; *Divine and McDonnell*, 2005]. In addition, at catchment scales, spiking systematically rainfall with artificial tracers is not within reach [but see *Rodhe et al*., 1996], and the spatial distribution of the tracer input is usually patchy. Although the linkage between hydrological tracer breakthrough curves and travel/residence time distributions is intuitive, proper interpretation requires multiple assumptions when dealing with systems naturally in unsteady flow conditions. Note that a common misunderstanding equates nonstationarity of the system's response to unsteady state conditions for inputs and output. Rather differently, stationarity refers to time invariance of the basic mechanisms that transform inputs into outputs whether in steady or unsteady state conditions.

Here we analyze the results of a 2 year experiment centered on the transport of fluorobenzoate tracers in a vegetated hydrologic transport volume. The specific tracers were chosen for the possibility of accurately singling out the relative concentrations of multiple injections. The experiment described in this paper aims specifically at tracking transport and release dynamics of solutes driven by hydrologic processes. For this purpose, we designed a controlled experiment in a large lysimeter, in order to restrict heterogeneous flow pathways to subvertical infiltration. Lysimeters have been extensively used in hydrologic research, in particular to study solute transport and evapotranspiration dynamics [e.g., *Bergström*, 1990; *Roth et al*., 1991; *Flury et al*., 1994; *Schoen et al*., 1999; *Beeson*, 2011, and references therein], because the rates and the concentrations of inputs and outputs can be monitored and the soil water storage can be estimated by accurately weighing the system. Compared to catchment experiments, this latest feature represents a major advantage for evapotranspiration studies owing to (water) balance closure. By injecting controlled fluorobenzoate tracer pulses in the system and by retrieving their breakthrough curves in the discharge, we infer travel and residence time distributions for a simple and yet highly dynamical system. Soil water storage and water deficits induced by evapotranspiration are particularly in focus as key factors controlling transport, as well as losses to plant uptake, microbial degradation, and residuals in soil. Evapotranspiration abstractions obviously operate preferentially at the surface and close to the roots. This could affect the transport of a tracer pulse, for example, by retarding its infiltration when a dry period characterized by high ET demand immediately follows the injection. In contrast, a large input volume occurring after the application of a tracer could flush the tracer pulse deeper in the soil, which would become unavailable or less prone to be selected by ET fluxes. In addition, the soil moisture cycles and how they propagate in the soil profile increase the complexity as they also affect water availability for ET and discharge (consider, e.g., a soil moisture below the wilting point). Adding tracer affinity for plant uptake, tracer losses can be largely driven by ET deficits and can thus be also influenced by environmental conditions. Microbial degradation is not necessarily as

intimately controlled by moisture conditions and ET as plant uptake does. Microbial degradation pathways are nonetheless often different between saturated and unsaturated conditions and specific conditions in the soil can prompt microbial activity (e.g., root exudates) and thus induce preferential degradation under certain circumstances, adding another nonlinear and nonstationary dimension to the hydrologic transport picture. Given the potential for a variety of loss pathways following the staggered solute injection, hypotheses on the modifications incurred in the travel and residence time distributions could then be tested by contrasting our experimental data.

This paper is organized as follows. Section 2 illustrates materials and methods. They include a description of the design of the experiment that entails multiple and replicated injections and of the system setup and its measurement system. Properties of the specific tracers adopted, five different fluorinated benzoic acids, and analytical procedures for their measurement are also discussed, leaving technicalities and ex post testing to Appendices. Section 3 presents our results, in the form of raw data which are publicly available as an attachment to the present paper and of mass recovery plots. Normalized and rescaled breakthrough curves are also produced to probe stationarity issues. Section 4 offers a discussion of the results and an outlook to catchment-scale transport experimentation. A set of conclusions closes the paper.

2. Materials and Methods

2.1. System Setup

The hydrologic control volume was placed within a large lysimeter (Figure 1) situated within the EPFL campus, in a 2.5 m deep fiberglass-polyester cylindric tank. The 1 m^2 open surface of the tank is at ground level and located in an open grass field equipped with meteorological stations. An underground chamber allows access to the bottom of the lysimeter where load cells record the weight.

A 50 cm layer of saturated gravel filter at the bottom of the tank is topped by a mono-horizon 2 m disturbed soil column. A geotextile mesh between the two layers prevents the soil to clog the gravel filter. The reconstituted soil is approximately 50% loamy sand obtained from a nearby construction excavation located in Denges (Switzerland) and 50% lacustrine sand with particle sizes from 0 to 4 mm (Lac Léman, Switzerland). The materials were accurately weighted and mixed with a cement mixer during the filling procedure. In order to ensure sufficient packing of soil and further compaction during the experiment, the soil was frequently soaked until saturation during the filling phase.

During the experiment, a steady water table is maintained at a constant depth of 2 m at the interface between the soil and gravel filter. The bottom boundary condition of the lysimeter is that of free drainage, as the excess downward flux recharging the gravel filter forces water out at the outlet placed at the bottom of the system. The outlet is connected to a PVC pipe maintaining the water table level through a siphon. The pipe outlet drains into a tipping bucket (Casella Measurement, UK) equipped with a double bucket of 8 mL resolution and a reed switch counter for discharge rate measurement. The tipping bucket is regularly calibrated by weighing the outflux in order to ensure unbiased measurements.

The lysimeter tank is supported by three concrete pillars topped with ring torsion load cells with a maximal load of 2.2 metric tons each (HBM, Germany) on which the tank pods stand. The electrical sensibility of the cells (2.85 mV/V) allows a continuous monitoring of the weight of the system with an accuracy up to 200 g (0.005%) of the total weight. The digital transducer of the load cells has a builtin infinite response (IIR2) electronic filter to remove noise notably due to vibration and wind. A filtered reading is stored every 20 s.

Local soil moisture content is measured by frequency domain reflectometry (FDR) probes (5TM from Decagon Devices Inc., USA) at four different depths in the soil column (25, 75, 125, and 175 cm). Three probes per depth were installed radially at equal distance from the center. A soil-specific calibration curve has been measured in the lab.

Two willows (*Salix viminalis*), 1.2 and 1.4 m in height (branch cuttings of a 2 year tree), were planted 8 months before the experiment started, with their roots extending to at least 70 cm in the soil column (data at time of setting). This species has been chosen because of its strong climatic resistance as it can withstand long periods of droughts as well as flooding. Willows have high transpiration rates and can thus potentially create substantial water demand in the system. A translucent gable roof made of polycarbonate built under

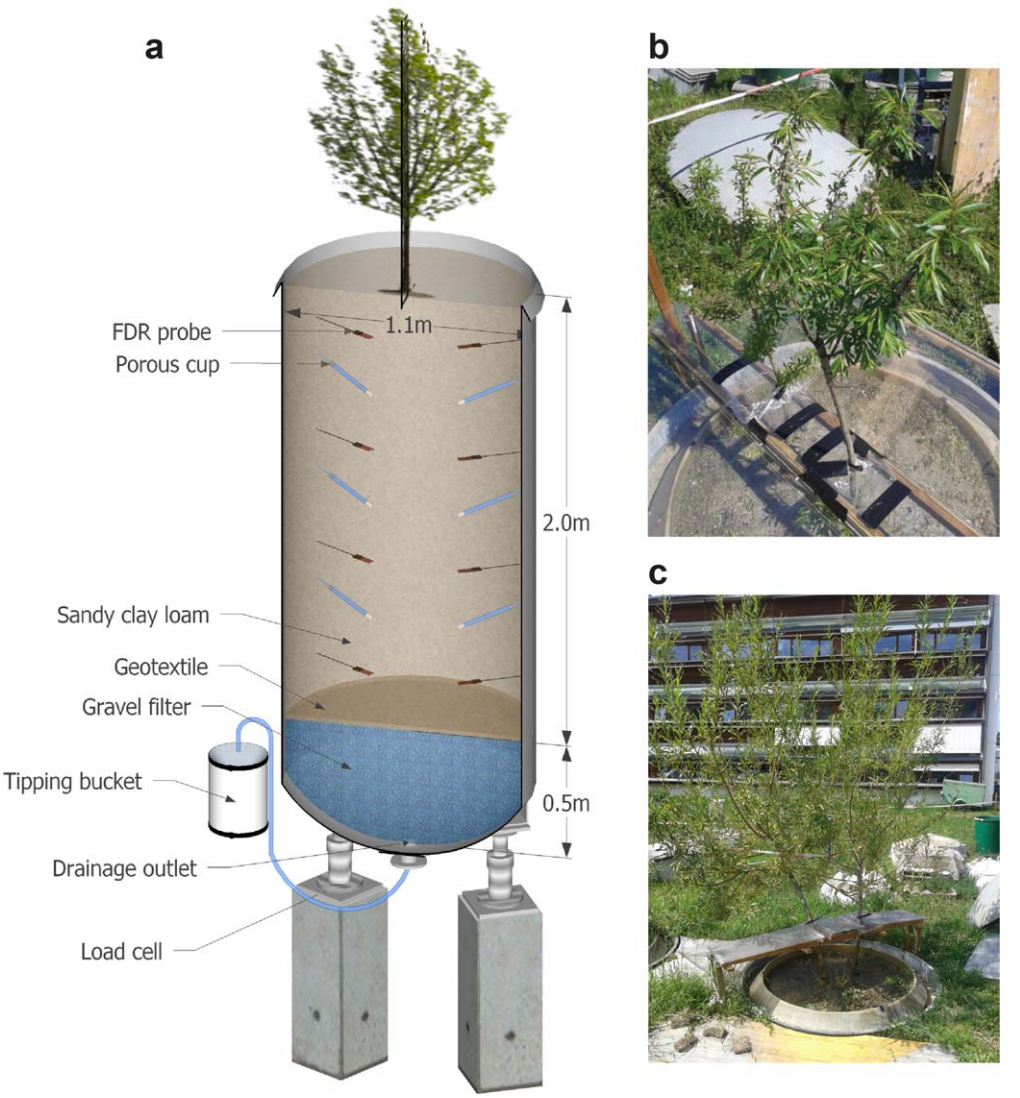

Figure 1. (a) General (to-scale) lysimeter scheme. An essential representation of the measurement devices is given. Note that a chamber placed underneath the lysimeter allows controls and measurement under any circumstance. Development of the willow tree (*Salix Viminalis*) in the lysimeter over the growing season: (b) 24 April 2013 and (c) 15 June 2014.

the trees canopy shields the lysimeter from natural precipitation but let the willow be exposed to the real climatic and light cycles (Figures 1b and 1c). Two openings on each side of the roof allow the crossing of an air draft and the evacuation of soil evaporation, besides allowing artificial water injection. The soil surface has been maintained bare throughout the experiment, and no organic layer could develop at the top of the column as the roof prevented accumulation of organic matter.

The evapotranspiration flux *ET* was derived from the mass balance, given the change in storage measured by the load cells, the input rainfall and the discharge output. Note that by evapotranspiration we term all combined evaporative/transpiration fluxes measurements lumped in a single variable outflux through the upper surface.

The system is equipped for soil water and discharge sampling. Soil water can be collected at three different depths in the soil (50, 100, and 150 cm) with three porous cups radially distributed per depth. The porous cups have a bubbling pressure of 1 bar and are connected to a vacuum circuit which is turned on at a relative pressure of −0.6 bar during 4–5 h to draw samples of about 10 mL in each porous cup from the soil matrix. Each sample is collected by an independent tube equipped with a manifold and is connected to a controlled vacuum system.

Table 1. Properties of the Fluorinated Benzoic Acids Used as Conservative Tracers

	TR1	TR2	TR3	TR4	TR5
Abbrev. name	2,5-DFBA	2-TFMBA	3,4-DFBA	2,6-DFBA	3-TFMBA
CAS No.	2991-28-8	433-97-6	455-86-7	385-00-2	454-92-2
Formula	$C_7H_4F_2O_2$	$C_8H_5F_3O_2$	$C_7H_4F_2O_2$	$C_7H_4F_2O_2$	$C_8H_5F_3O_2$
Mol. weight (g/mol)[a]	158.1	190.1	158.1	158.1	190.1
Solubility (g/L)[a]	745	1000	266	1000	802
pK_a[b]	2.87	3.17	3.43	2.42	3.50
LOQ (μg/L)	7.0	3.0	10.0	7.0	5.0
Intern. std.	Deutered	NA[c]	Deutered	Deutered	NA[c]

[a]SciFinder®, Chemical Abstracts Service: Columbus, OH. Calculated using Advanced Chemistry Development (ACD/Labs) Software V11.02 ([copyright] 1994–2013 ACD/Labs).
[b]*Serres-Piole et al.* [2011].
[c]Not available at time of experiment.

Discharge samples are collected at the tipping bucket outlet. The effluent is directed to a solenoid valve switching the flux either to the sink or to a fraction collector (Amersham Biosciences AB, Sweden) when a sample is needed. A LabVIEW™ program connected to a data acquisition system (CompactDAQ, National Instruments) is used for calculating the flow rate based on the bucket tilts read by the reed switch of the tipping bucket. It also controls the valve position and increments the fraction collector after a sample has been taken. The program interface provides user-defined parameters and allows time or flow-based sampling schemes.

A meteorological station located 5 m away from the installation records air temperature, air humidity, wind direction and intensity, incoming radiation, and soil temperature at 15 min intervals.

2.2. Selection of Suitable Tracers

The goal of the experiment is to tag and trace selected water inputs. For this purpose, a given volume of water from a given pulse has to be independently labeled. Because the discharge flux is assumed to be, at every given time, a mixture of water originating from inputs and thus characterized by a specific age structure, it is continuously analyzed for the labeled water. The detection of the label hence suggests how water from a marked rainfall event contributes to the discharge flux.

As tracers, we have chosen fluorinated benzoic acids (FBAs) that were argued to be convenient for hydrologic tracing in soils [e.g., *Jaynes*, 1994]. Different species of FBAs exist, depending on the number and position of fluoride ions on the aromatic ring. Several FBA compounds have been reported as useful nonreactive water tracers, often described to have similar reactive properties as Br^- [e.g., *Bowman and Gibbens*, 1992; *Jaynes*, 1994; *Kung et al*., 2000; *Mortensen et al*., 2004]. FBA derivatives are anionic at neutral to basic pHs and have negative-log dissociation constants (pK_{as} less than 4.0), which limits sorption effects in soil [*Bowman*, 1984; *Stetzenbach et al*., 1982; *Bowman and Gibbens*, 1992; *McCarthy et al*., 2000]. To date, few studies exist that reported chemical and microbial degradation of fluorinated compounds [*Misiak et al*., 2011]. Plant uptake of some fluorobenzoic acids has been reported [*Bulusu*, 1995; *Bowman et al*., 1997]. Analyses of soil and plant extracts reflected an uptake ranging from 0 to 50% depending on the compound and plant species and suggest possible metabolism within the plant material [*Bulusu*, 1995]. Affinity for plant uptake is further assessed during this experiment via the analysis of willow twigs and leaves. Upon verification of commercial availability, reported low reactivity in saturated soils and chemical analysis capabilities, five species have been identified as suitable for the current experiment: 2-(Trifluoromethyl)benzoic acid (2-TFMBA), 3-(Trifluoromethyl)benzoic acid (3-TFMBA), 2,5-Difluorobenzoic acid (2,5-DFBA), 2,6-Difluorobenzoic acid (2,6-DFBA), and 3,4-Difluorobenzoic (3,4-DFBA). All compounds were purchased in salt powder at a minimum purity of 99% from Fluorochem (Hadfield, UK). Their chemical properties are listed in Table 1.

We performed a column leaching test in order to confirm the absence of significant sorption for the five selected chemicals on the same soil used in the lysimeter (Appendix A). In addition, plant and soil extracts were analyzed after the experiment was terminated to examine whether FBAs had been accumulating in the biomass. Microbial degradation was probed by measuring Fluoride concentration (a by-product of any FBA breakdown) in a selection of discharge and soil water samples (Appendix B).

2.3. Tracer Analysis

FBAs can be analyzed using different methods [*Stetzenbach et al*., 1982; *Lasa and Åšliwka*, 1990; *Galdiga and Greibrokk*, 1998]. Liquid chromatography coupled with mass spectrometry appears to give the best analytical sensitivity [*Dalian and Ronen*, 2001; *Juhler and Mortensen*, 2002]. The FBAs were therefore quantified by LC/MS-MS (Acquity® TQD, Waters). The limits of quantification obtained with this procedure were obtained during the calibration with standards and vary between 3 and 10 μg L^{-1} according to the compound (see Table 1). Three of the five compounds have deutered internal standards (2,5-Difluorobenzoic-d3 Acid, 2,6-Difluorobenzoic-d3 Acid, and 3,4-Difluorobenzoic-d3 Acid) purchased at EQ Laboratories GmbH (Augsburg, Germany). Furthermore, 0.11 mL of a preparation containing 120 ng mL^{-1} of deuterated standards diluted in ultrapure methanol was added in all the vials containing 1 mL of sample prior to the injection. A calibration procedure was performed to validate the analytical method and discard potential matrix effects.

2.4. Tracer Sampling

Discharge water was sampled using a flow-proportional sampling device. A 20 mL sample was taken every 1–3 L of cumulative discharge flow, depending on the time during which the system is left unattended and the number of sample bottles in stock on the fraction collector tray. Soil water was also sampled every 2–3 days at each depth. The samples were filtered by 0.45 μm hydrophobic syringe filters with GMF/PP membranes (BGB Analytik AG, Switzerland) as soon as possible and stored at 4 °C in prior to analysis.

2.5. Rainfall and Tracer Applications

The rainfall series was constructed using a marked Poisson process with interarrival time λ and mean rainfall depth α, as proposed for daily rainfall in the classic approach by *Rodriguez-Iturbe et al*. [1999]. The two parameters of the rainfall distribution were arbitrarily defined in order to maximize the coefficient of variation of the hydrologic travel time in the vadose zone and to minimize the ensuing mean travel time for the entire duration of the experiment. For comparison, we have estimated mean travel times using the approach of *Harman et al*. [2011], who has calculated the coefficient of variation of mean travel times as a function of two lumped parameters using a simple piston displacement model. One parameter (γ) subsumes soil properties and the type of climate. Hence, given the soil properties of the lysimeter and the estimated potential evapotranspiration for a willow crop [*Persson*, 1995; *Schaeffer et al*., 2000; *Guidi et al*., 2008], the interarrival time and the mean rainfall depth were set to 0.67 day^{-1} and 20.3 mm, respectively. Multiple rainfall sequences with selected parameters were generated.

Five rainfall events predicted to drive significantly different travel times were selected within a time span of 1 month. Each rainfall event was labeled with a different FBA tracer. Two of these tracers were simultaneously reinjected 10 months later, once the outflow concentrations of all previously injected tracers were found below the detection limit. This provided two additional measurements of solute travel times which prove particularly valuable to test whether the different tracers are subject to reactivity and/or degradation processes. Replicated, compound-specific measurements of breakthrough curves for two tracers have thus been gathered. We selected the tracers with the highest and lowest recovery ratio after the first injection (2,6-DFBA and 2,5-DFBA, respectively), in order to additionally establish whether their disparity in the breakthrough is not only an artifact of different degradation extent. Discharge and soil water concentration monitoring lasted until the tracer concentration decreased below the detection limit (July 2014).

"Rainfall" events were generated manually in the lysimeter system as quasi-instantaneous pulses—poured from a watering pot directly onto the soil surface. For the labeled rainfall events, a primary tracer stock solution was prepared for each FBA by dissolving the targeted mass of powder in 20 mL of ultrapure methanol. The stock solution was further diluted in the volume of water corresponding to the labeled rainfall event and immediately injected in the lysimeter. Resulting tracer concentration in the rainfall water varies in the range of 90 to 230 mg L^{-1}. The system was conditioned with a chosen rainfall pattern during 2 months before the injection of the first tracer, so that the water content profile in the soil column can be assumed to be consistent with the type of climatic forcing simulated. The five selected tracers were all injected during the first month of the experiment, starting on 17 April 2013. This relatively short-period limits the overall evolution of the system between the five injections, so that all tracers would have faced roughly the same system states. This condition restricts the origins of the heterogeneity in the observed fate of the five tracers to differences in the external forcing (precipitation and evapotranspiration) during the early stages of their hydrologic journey. It is to be noted that the mass of each tracer was adjusted to obtain a concentration in

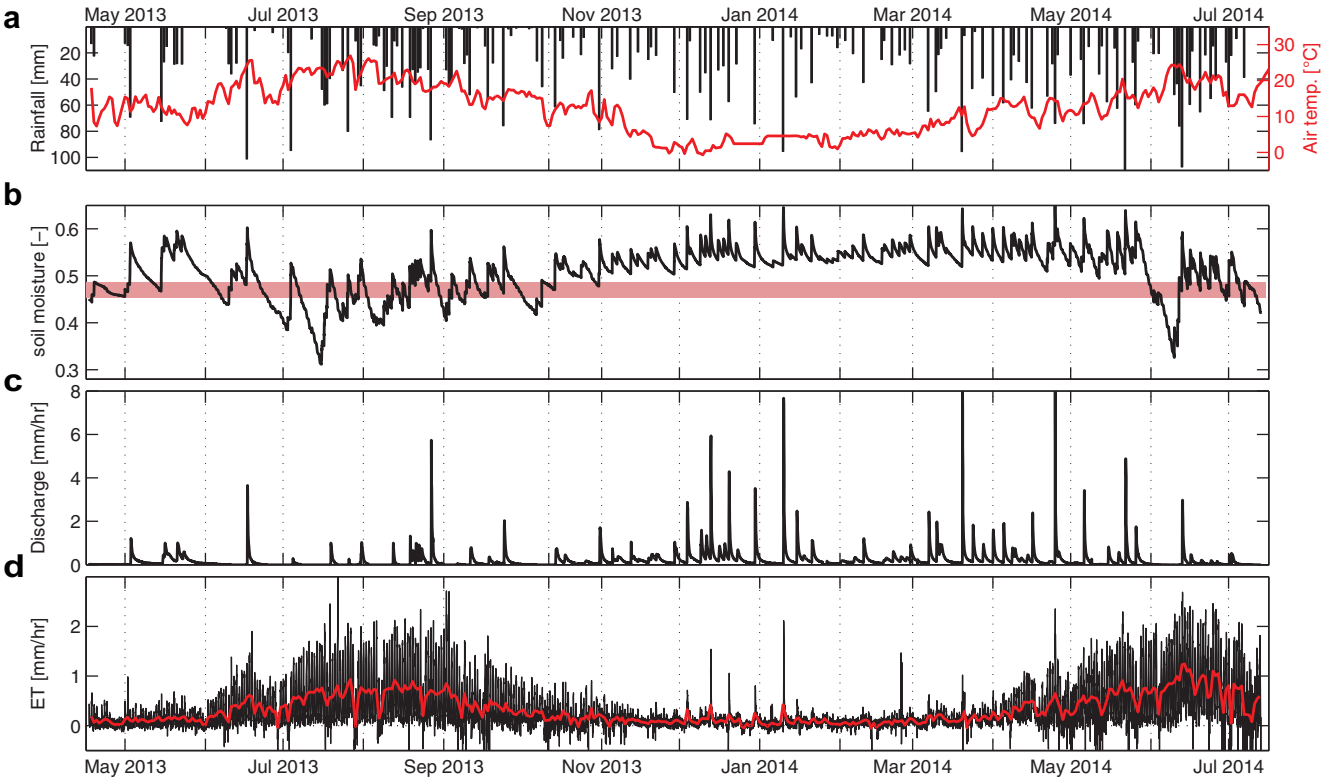

Figure 2. Input and output fluxes of the system during the selected experiment period. (a) Daily rainfall events and mean daily temperature (red). (b) Soil moisture, i.e., relative fraction of saturated soil porosity $\in (0, 1)$. The red band shows the lower and upper quartiles of soil storage that triggers discharge flux. (c) Discharge rate at the outlet. (d) Hourly (black) and mean daily (red) evapotranspiration flux.

the batch injection volume of the order of 0.1 g L^{-1}, in order to avoid concentration effects between each tracer injection.

3. Results

3.1. Hydrological Fluxes

Figure 2 summarizes the measured in and out-fluxes and the dynamics of soil moisture, here shown at an hourly time scale. It can be observed that soil moisture (Figure 2b) responds to rainfall patterns (Figure 2a) by producing variable interevent moisture conditions constrained to a relatively narrow range. This is also related to the discharge response (Figure 2c) which is only triggered when the overall soil moisture crosses a threshold (red band in Figure 2b). Of the cumulative rainfall during the observed period, 39% (2243 mm) was discharged at the outlet whereas 61% (3454 mm) was either evaporated at the soil surface or transpired by the willow. Values of ET rates that might appear exceedingly high are explained by the fact that willow crown and overall canopy occupy a surface much larger than the lysimeter.

A large rainfall input (83 mm) occurring at relatively wet antecedent conditions triggered the maximum observed discharge rate Q up to 12 mm h^{-1} on 25 April 2014, 3 h after injection (Figure 2). Large discharge flow occurs more frequently in winter, when soil moisture is consistently above 0.5 due to limited ET abstractions. As shown by the event of 26 August, however, a large rainfall event could drive discharge rates above 4 mm h^{-1} even in summer conditions. Antecedent rainfall is in general necessary in order to compensate the large ET demand credited by the large canopy and to increase soil moisture throughout the profile. Hence, not only the overall storage but also the spatial heterogeneity of the water content is a key factor controlling the discharge rate, a feature commonly observed in real catchments [e.g., *Hrachowitz et al.*, 2013].

The *ET* signal at hourly time scale mirrors daily and seasonal cycles of climate and vegetation (Figure 2d). Unphysical negative values were observed when *ET* was lower than the noise level of the load cells. It is

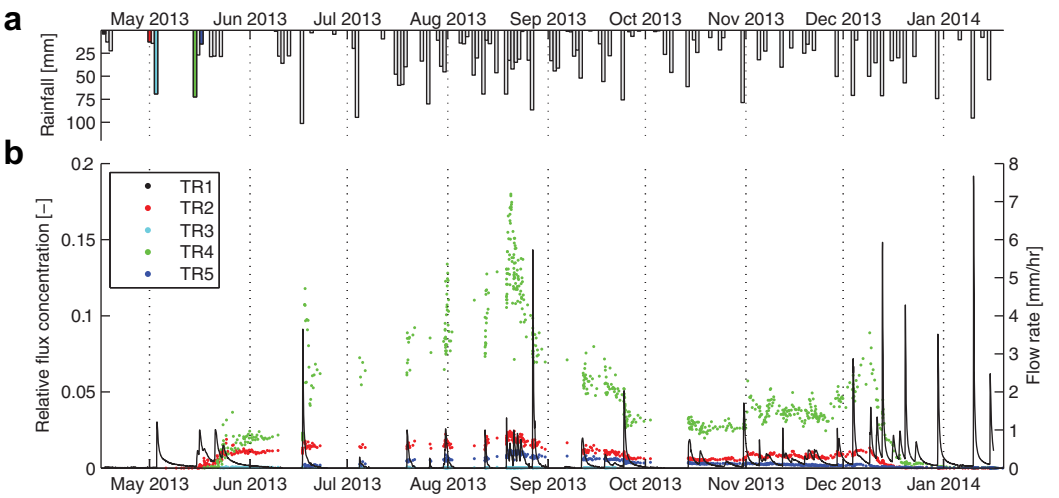

Figure 3. Results of the tracer experiment, for the sequenced injection of 2013. (a) Sequence of applied precipitation with tracer-marked events (colored). (b) Tracer breakthrough curves in the discharge expressed in relative concentration to their respective input (colored dots) and flow rate (black line).

reasonable to assume that nightly surface evaporation and plant transpiration were negligible in early spring, when the air temperature T and plant activity were low (say, $T \leq 10°C$). The observed signal confirms such assumption, as *ET* values are found close to zero between 8 P.M. and 9 A.M. from the experiment start until early June and from November onward. The daily evapotranspiration varies between 3–5 mm d^{-1} in spring and more than 20 mm d^{-1} in summer. Corrected for the ratio of the crown area of the actual canopy and the lysimeter surface, this represents about 1.5–2.5 mm d^{-1} in spring and about 10 mm d^{-1} in summer. The literature reports transpiration typically around 5 mm/d during the growing season of young willows [*Persson*, 1995; *Schaeffer et al*., 2000]. However, *Guidi et al*. [2008] measured ET values up to 14 mm/d in late summer for a fertilized willow with stem size reaching 300–400 cm. Moreover, as the soil surface of the lysimeter is covered by a translucent roof and well ventilated with large side openings, we speculated that our installation may have acted as a greenhouse (under the willow canopy) by increasing soil surface evaporation through heating. The gradual augmentation of *ET* between the beginning of June till the end of July corresponds both to an air temperature increase from 10 to 27°C and to an important growth of the two willow stems of 100 cm in height (both 250 cm on 24 July). The sudden decreases of the *ET* flux visible in Figure 2d on a few occasions (e.g., 29 June, 29 July, and 7 August) corresponds to important rapid temperature drops of 5–10°C. The simultaneous noise increase in the signal can be explained by the weather degradation often characterized by strong precipitation that generate unexpected water inputs in the system by flowing through the roof chinks. The data were averaged and corrected to produce a positive definite time series of abstractions as shown in Figure 2.

3.2. Tracer Dynamics and Fluxes

Figure 3a shows the precipitation sequence. It emphasizes the events that were marked with a specific tracer. For the ease of reference throughout the paper, 2,5-DFBA is referred to as TR1, 2-TFMBA as TR2, 3,4-DFBA as TR3, 2,6-DFBA as TR4, and 3-TFMBA as TR5. The tracer breakthrough curves (Figure 3b) display the measured concentrations in the discharge samples normalized to the initial concentration of the injection batch volumes for each tracer. The maximum peak relative concentration was recorded for TR4 at 0.18 on 21 August, 98 days after its injection. The relative peak concentration for TR2 and TR5 were also measured on the same date (112 and 96 days after their injection), but at a much lower concentration (0.242 and 0.012, respectively). In contrast, TR3 peaked only 46 days after injection where the maximum relative concentration was only 0.001. TR1 was never detected in the discharge, but only in soil water samples, as described below. At the end of the first injection period (January 2014), the concentration of all five tracers in the outflow was below the analytical limit for quantification.

The total mass recovered in the outflow with time is shown in Figure 4b by the shaded area. Considering that TR4 was injected 15 days after TR2 and that the initial mass of TR4 in rainfall was more than 2.5 times

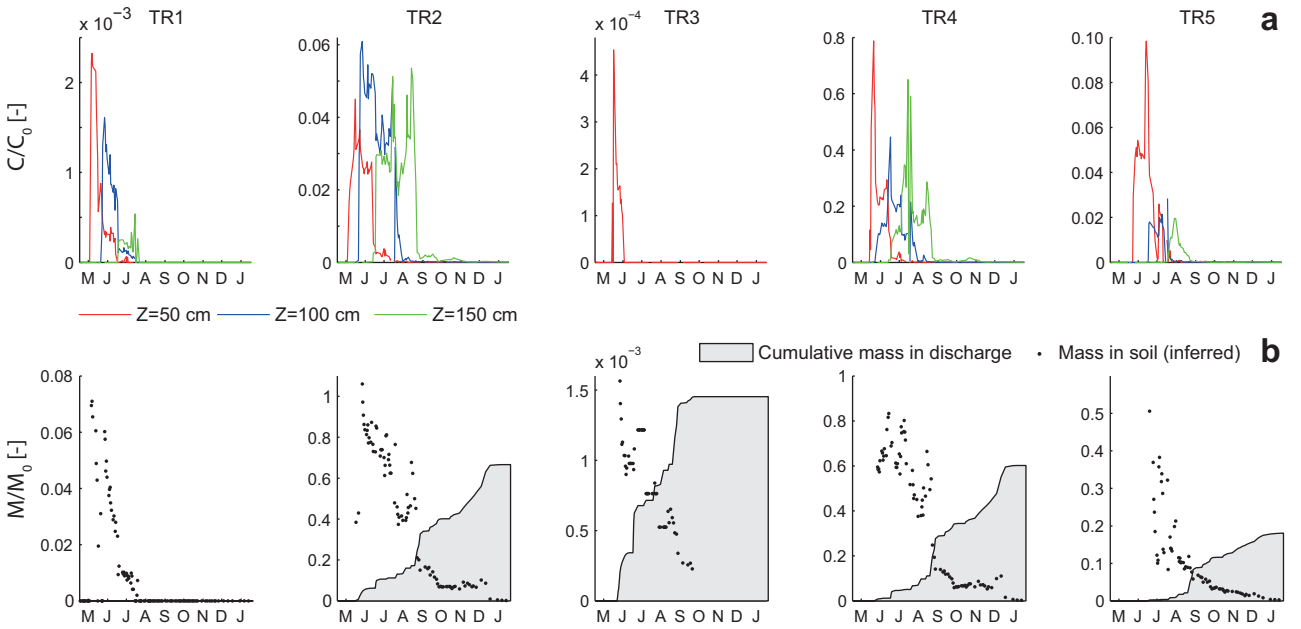

Figure 4. Tracer data in the soil water for the sequenced injection of 2013. (a) Temporal evolution of the relative concentration of each tracer in the soil water at three control planes distributed in depth (concentration average of all soil water samples available per depth). (b) Estimation of the relative total mass of each tracer in the soil column and gravel filter (points) with cumulative tracer mass having exited the system through discharge (gray area).

the initial mass of TR2, the export patterns of TR2 and TR4 are synchronized, and the amount of tracer mass exported during each discharge event is similar for the two compounds. In contrast, TR5, injected only 2 days after TR4 (and with a similar initial mass as TR2), shows a more attenuated export dynamics, with only about 18% of its initial mass recovered in the discharge, whereas TR2 and TR4 were recovered at 67% and 60%, respectively. Less than 0.2% of the mass of TR3 was recovered in the discharge.

Owing to the sampling of soil water at the control ports placed at three different depths, a concentration profile in time inside the soil column can be estimated for each tracer (Figure 4a). Even if the data available are spatially discrete, they show interesting features. For instance, even if TR1 has not been detected in the discharge (see Figure 4b), it was measured in the soil water samples during 3 months at detectable concentrations (in the order of 0.1% of the initial concentration of the input) at all depths. In contrast, TR3 was measured in the discharge samples (0.1% of total recovery), but it was only detected in soil water samples at 50 cm at a maximal concentration about 1 order of magnitude lower than TR1.

The behavior of the water pulses labeled with TR2 and TR4 proves very different from TR1 and TR3, in that the total mass recovered is much higher for the first two (60–70% against less than 0.2%, respectively). The total tracer mass in the system (black dots in Figure 4b) has been calculated by assessing the mean concentration for each control plane (then averaging on all planes) and multiplying it by the current water storage. We observe that initially, this estimation captures the entire input tracer mass for TR2 and TR4, whereas only 50% of the input mass of TR5 is measured and less than 1% for TR1 and TR3 (note that the *y* axis varies by orders of magnitude between the plots). This method may actually underestimate the mass in storage due to the low-depth resolution of concentration measurements and the assumption of homogeneously distributed soil moisture, especially if the tracer pulse volume is small (e.g., if the pulse is temporarily be located outside the probes' volume of influence, as in the case for the TR1 data in May). However, one notes that the input volume of TR3 was very large (77 L), and yet the maximal relative concentration observed at the upper depth is 0.04, the lowest value measured for all tracers. The estimated TR3 mass at this depth is later recovered in the discharge, which suggests that most of the mass loss occurred in the early phase of the breakthrough and at shallow depths. In contrast, TR1 is detected at all depths and in higher concentration, even though the input volume was much smaller (5 L) and therefore more prone to bypass the localized sampling points. As for TR1, only a fraction of the input mass of TR5 is detected early in the soil water (about 40%, less than 10% for TR1). The overall concentration decreases considerably with depth for the

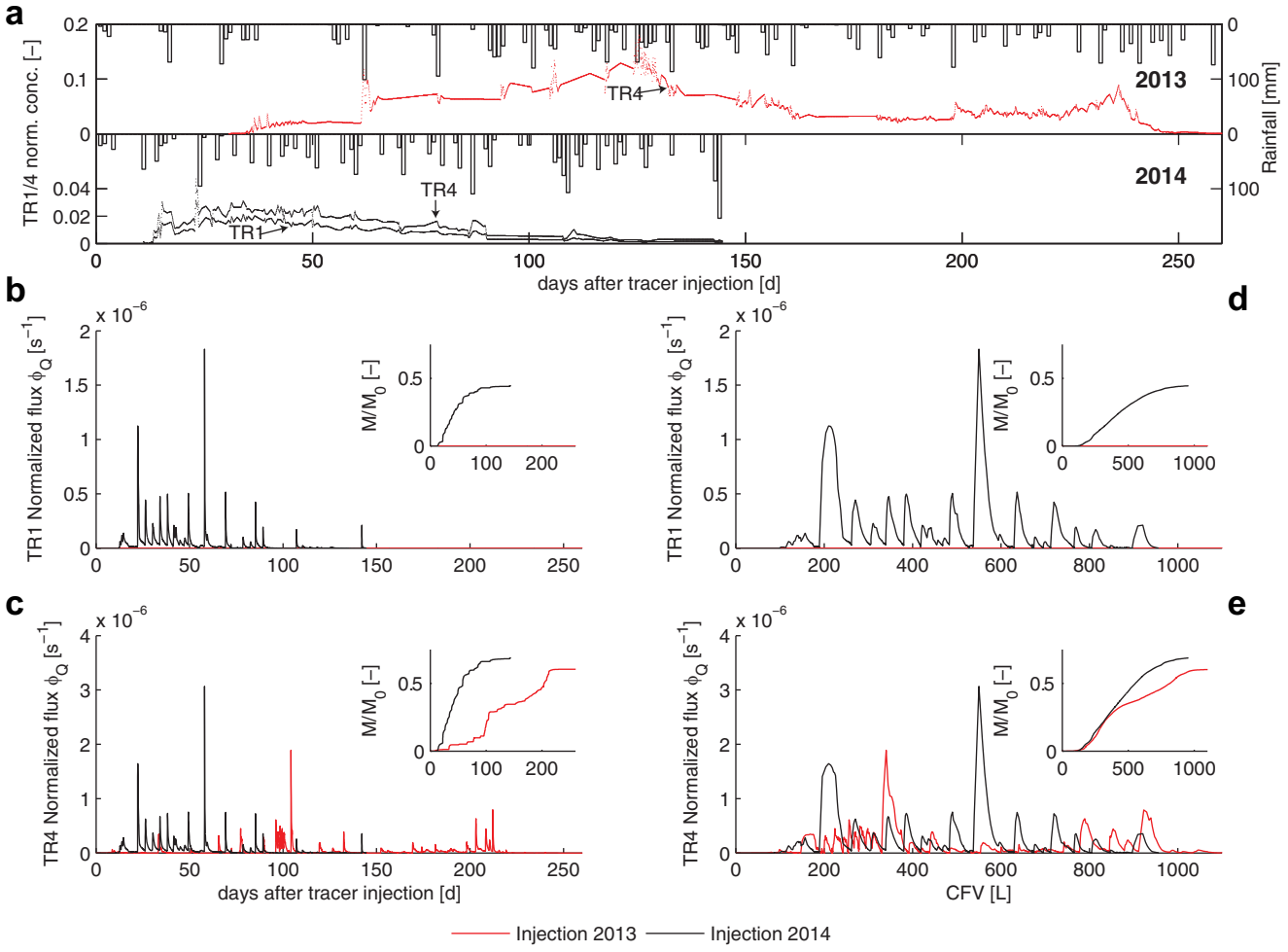

Figure 5. Comparison of the discharge concentration and mass fluxes between the validation tracer test conducted in 2014 (with simultaneous injection of TR1 and TR4, represented in red) and the sequenced injection in 2013 (only TR1 and TR4 are shown, represented in black). (a) Concentration breakthrough of the (top) 2013 injection and (bottom) 2014 injection, with their respective rainfall sequence (bars). The mass flux and cumulated mass recovery (inset) for (b) TR1 and (c) TR4 plotted versus the elapsed time since injection. Note that, TR1 was not detected at all during the 2013 injection. (d and e) The mass flux of TR1 and TR4, but plotted versus the rescaled time since injection, proportional to the volume discharged *CFV*.

two tracers, suggesting a degradation or uptake of the tracer. In comparison, the overall concentration per depth for TR2 and TR4 does not seem affected by such a reduction. Finally, the TR5 pulse shows intermediate infiltration and export patterns between TR1/TR3 and TR2/TR4. About 20% of the initial mass has been retrieved in the discharge and the estimated mass in the soil column has never exceeded 50%.

When injected simultaneously (like in the second validation injection from February 2014), TR1 and TR4 (least and most recovered tracers during the first test, respectively) demonstrate identical release dynamics even if the signal of TR1 is mitigated compared to TR4 (black lines in Figure 5a). The mass recovery of TR1 was 45% at the end of the sampling period, and 69% for TR4. In contrast, the recovered TR4 mass during the first injection after the same cumulative discharge volume was 60% (Figure 5, insets).

Further interpretations of the mass recovery are contained in Appendix B following ex post analyses of biomass and samples.

The various degrees of mass recovery of the tracers indicate that they are all subject to degradation or removal processes, possibly at various extents specific to each tracer. This restricts our analysis to hydrological transport of the three tracers that were significantly retrieved (TR2, TR4, and TR5). Because two FBAs did not appear in discharge samples after the first injection, interpretation of the results in terms of reactive hydrologic transport emerged as necessary to explain the observed discrepancies. The comparison of the

breakthroughs of the same tracer injected twice at different times (TR1 and TR4) dismisses instead the specific reactivity issue, and is therefore presented first in the discussion (time displaced injections). This sheds light on the interpretation of the multiple tracer injection. Finally, inferences on the reaction processes affecting the FBAs in this experiment are discussed in the last section, based on the tracing results and complementary testing presented in the Appendices A and B.

4. Discussion

4.1. Temporally Displaced Injections

The reinjection of TR1 and TR4 provides a demonstration on the effects of the hydrologic forcing on the solute transport features. In contrast to the short-time injection sequence of multiple tracers of 2013 (discussed below), we can compare here (Figure 5a) two breakthroughs of the same tracer injected at different times and dismiss potentially distinct reactive behaviors among the tracer species. Therefore, disparities in terms of concentration and load dynamics for a specific tracer only result from the different hydrologic forcing and the sequence of conditions experienced by the system. Figure 5a shows the precipitation sequence and the concentration breakthrough of TR1 and TR4 in 2013 (top figure) and 2014 (bottom figure). For TR4, the concentration dynamics prove substantially different between 2013 and 2014, both in terms magnitude (note the *y* axis scale) and shape. The duration of the breakthrough is about 1.5 times longer in 2013 than in 2014 and reach a maximal relative concentration almost 4 times larger than in 2014.

Figure 5c shows the normalized mass fluxes of TR4 for each injection. In this case, the magnitude of the tracer load is comparable between the two injections, meaning that the water discharge was generally greater in 2014 to compensate lower concentrations in producing similar mass exports. This is especially true for the early phases of the 2014 injection, because it took place in late February (mid-April in 2013) when temperature and plant activity were low and ET losses relatively small leading to increased discharge responses for a specific rainfall volume. In the case of TR4, we clearly observe nonstationarity of the system's ability to transfer inputs into outputs both in terms of concentrations and mass fluxes. The different precipitation pattern between 2013 and 2014 would of course induce a different timing of the tracer export events. However, in the case of an invariant transfer input-output function, the tracer responses would appear much more alike, and the cumulative recovery curves (Figure 5c, inset) would evolve similarly. Instead, we observe that the major part of the tracer injected in 2013 is recovered after more than 100 days, whereas the 2014 pulse is recovered much earlier.

ET plays a central role on the hydrologic and solute response. Part of the rainfall inputs never reaches the bottom drainage of the system to produce discharge, but is rather withdrawn by the vegetation and transpired or is evaporated at the soil surface. The consequences of ET on solute transport are evident as it obviously affects the water balance (and therefore the discharge response for a rainfall event). However, ET also conveys more intricate aftermaths on internal mixing, because it operates on different pools of water (and consequently water characterized by different ages) than discharge does. Note that this represents an important issue on reactive transport as the exposure time to various degradation/removal processes is altered (discussed in section 4.3).

In an effort to investigate the nonstationarity solely induced by the variability of the water balance (i.e., the effects of the variable precipitation influx and variable ET water outfluxes), we have rescaled the tracer fluxes using the cumulative flow volume (CFV) $t \rightarrow \int_{-\infty}^{t} Q(x)dx$ as independent variable (Figure 5e). With this approach, the differences in the rainfall structure and ET deficits between the 2013 and 2014 injection are implicitly integrated in the dynamics of the tracer mass outflux curve, as the metrics used is the effective hydrologic outcome of the system exposed to the specific environmental forcing of each injection year. It had been argued, in fact, that this choice yields stationary travel time distributions even under unsteady flow conditions provided that changes in the storage $S(t)$ are not major [*Niemi*, 1977]. The result is plotted in Figure 5e. It is not surprising that the mass load exported per drainage volume unit discharged evolves, but one might have expected a unimodal shape, picturing the progressive arrival of the tracer front (i.e., the tracer concentration in the discharge water increases gradually) until the mass pulse's centroid is reached followed by a decrease until all tracer is discharged. Instead, we observe here multiple peaks corresponding, in terms of chronological time, to large discharge events. This implies that the composition of the discharge constantly evolves sampling water from different pools. The latter point suggests that when precipitation

occurs, soil moisture increases and is redistributed, connecting water parcels that were previously hydrologically isolated as customary in macropore flow in unsaturated soils. ET also plays a key role, as it samples water from pools that can be different than those accessible to the discharge, especially in a lysimeter installation. This is particularly evident for evaporation, which arguably samples water mostly at shallow depths, thereby changing both the availability of water and the hydrologic connectivity in the system. We show in Figure 5c that almost no tracer outflux occurs between 100 and 200 days after the 2013 injection, which corresponds to the summer months (July–September) when ET was maximum. Although the ET deficit was notable, the multiple rainfall events generated during this period have prompted a nonnegligible discharge (about 300 L corresponding to CFV values between 400 and 700 L in Figure 5e). Whether or not the tracers may undergo plant uptake, the fact is that TR4 was still in the volume during this period as TR4 export increased again significantly later on, but was not readily accessible for discharge because of the specific conditions in the system.

The reinjection of TR1 is less explanatory than TR4 in deciphering the key features of bulk transport, as no breakthrough was observed for this tracer in 2013. Nevertheless, this experiment illustrates an important implication of nonstationary transport when a reactive solute is at stake. The first injection of TR1 objectively dismissed any premise of nonreactivity, as the entire tracer input mass disappeared in the system and was never observed in the discharge samples. In contrast, the reinjection of the tracer in 2014 resulted in a total mass recovery of 45% (Figure 5b, inset), only slightly lower than TR4 which was injected simultaneously. This discrepancy emerges because the exposure time of the tracer to the potential degradation/removal processes changes significantly between 2013 and 2014 as a consequence of nonstationary transport and mixing. As the processes that are involved in the tracer removal (discussed in section 4.3) may entail complex dynamics like, e.g., selective plant uptake or microbial degradation controlled by environmental conditions, it proves difficult to relate the mass loss with the hydrological and environmental conditions encountered by the system. This issue is further analyzed and discussed in the framework of a modeling exercise presented in a companion paper [*Queloz et al.,* 2015].

4.2. Sequenced Multiple Tracer Injections

In 2013, five tracers have been injected sequentially within a 1 month period. The initial conditions were thus variable and a different forcing occurred for each tracer shortly after their injection. Nevertheless, as the mean travel time until the tracers exited the system through discharge was much longer than for the 1 month injection period, the tracers experienced mostly the same system's states during most of their transport in the soil. Despite similar overall forcing, we observe very different tracer responses (Figure 3). The total mass recovery ranging between 0 and 67% suggests that removal/degradation processes have occurred and affected the tracers to various extents. However, the simultaneous reinjection in 2014 of TR1 and TR4—a priori two dissimilar tracer in terms of reactivity given the results of the 2013 injection—shows fully synchronized discharge concentrations, with the relative concentration of TR4 about 1.5 times larger than TR1 during almost the entire breakthrough (Figure 5a). Hence, TR1 seems more prone to degradation or uptake. In the absence of hydrologic differentiation, however, the effects of each specific tracer dynamics are mainly limited to the magnitude of the signal rather than to its timing.

All things considered, hydrologic processes exhibit a key role in explaining the radically different behaviors of the five tracers injected in 2013. In Figure 6a, the fluxes are normalized and the time axis is adjusted to the injection time of each tracer, respectively. Whereas, the signals of TR2 and TR4 (separated now with a 14 days lag equal to the time that separates their injection) are similar most of the time, we note that they only diverge between 0 and 56 days. This is even clearer in Figure 6c where time is rescaled in terms of CFV (see section 4.1), as the signals become similar only after 220 and 300 L for TR4 and TR2, respectively. Therefore, the comparison of TR2 and TR4 reveals that their availability for discharge is distinct in an early phase after their injection, but becomes equivalent after some time (for example, the discharge event occurring 33 days after the injection of TR4 and 47 days after the injection of TR2 mobilizes proportionally more TR2 than TR4, whereas the following discharge events mobilize TR2 and TR4 equally).

TR5 was recovered at a much lower ratio than TR4 and TR2 (18% against more than 60%), yet the normalized flux in Figures 6b and 6c exhibits common features of TR5 with the other tracers. The early discharge events that generate mass export for TR2 and TR4 do not affect TR5, whose breakthrough begins only after 170 L CFV. As soon as TR5 is detected in the discharge, the mass flux shows the same shape as for the other

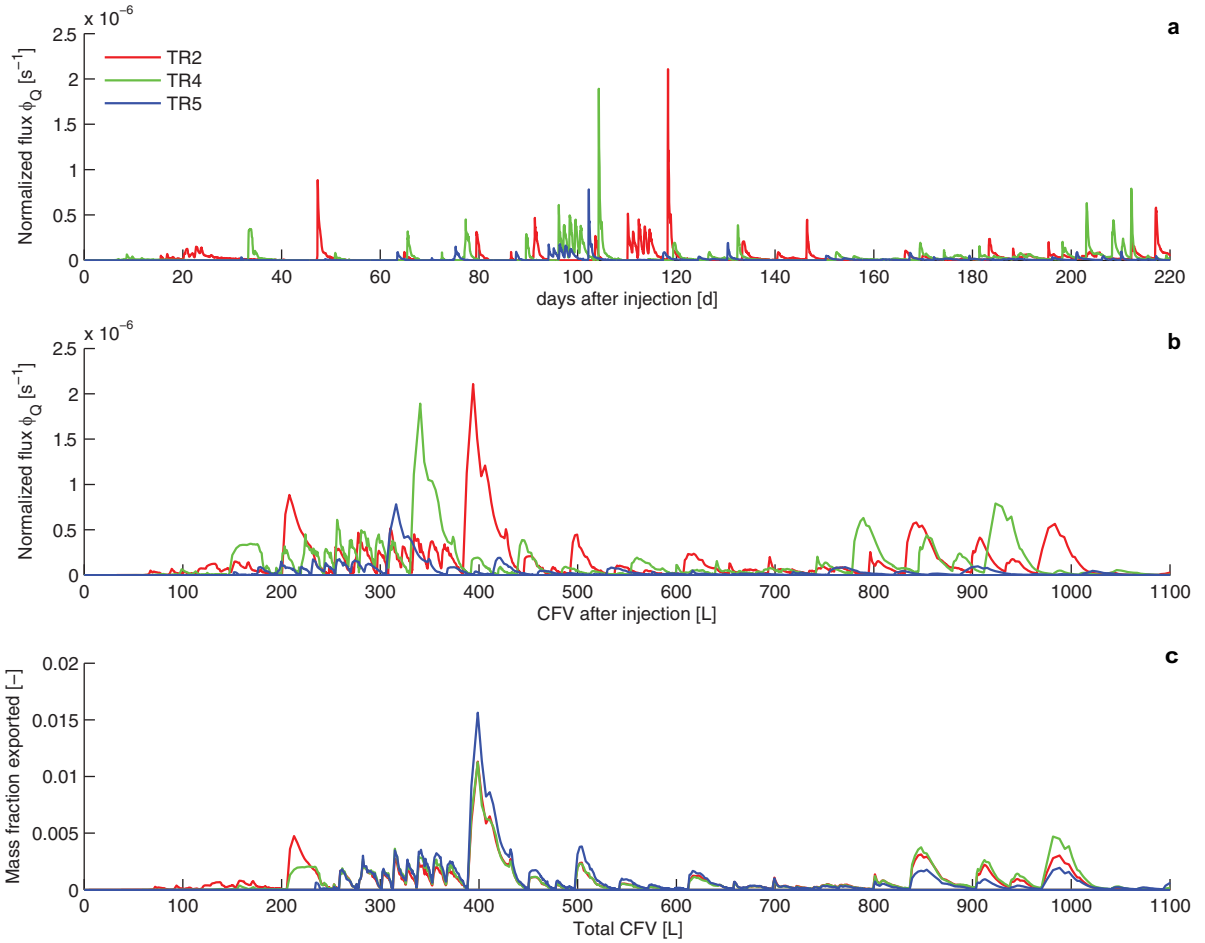

Figure 6. Summary of results of the transport experiment. (a) Tracer-normalized flux ϕ_Q plotted versus chronological time t; (b) tracer-normalized fluxes plotted versus the rescaled elapsed time since injection, proportional to the volume discharged $CFV = \int_{t_i}^{t} Q(x)dx$. (c) Fraction of the total mass recovered exported per cumulative flow volume (CFV) discharged since the injection of TR1.

two tracers. Its magnitude is about half those of TR2 and TR4, but if the signals of each tracer are normalized by their maximum value, we observe that the relative magnitude of the TR5 signal is identical with the others until about 600 L CFV, and decreases afterward. Hence, the weaker outflux of TR5 is due to mass loss that occurred early in the system's transport, i.e., before the beginning of its breakthrough. These data are not sufficient to identify whether TR5 is degraded or removed by plant uptake from the system, but the similarities of the relative signals suggest that if it is the case, all tracers (TR2, TR4, and TR5) are affected in a similar manner. The final decrease of TR5 outflux relative to the TR2/TR4 arises because TR5 is almost completely removed from the system.

Two main outcomes of the measurements of TR2, TR4, and TR5 are worth discussing further. When solute pulse injections are operated sequentially under different environmental conditions, we observe similar breakthrough dynamics until the entire solute mass has exited the system. This is because each single discharge event mobilizes the different solutes equally and thus the relative quantity of solute exported during one event is the same for all compounds. However, this only occurs after a suitable period following the solute injection, while the solute spreads in the system. It appears that most of the differentiation between the various injections (and various tracers) in terms of mass loss occurs during this period. Unequal reactivity of the tracers cannot be ruled out, but Figure 6c suggests that the accountable degradation processes arise soon after injection. Consequently, as the hydrologic conditions during early transport phases are different for each tracer, they may also influence the degradation processes and induce the variability observed among the tracers. This issue is further discussed in the next section and in a companion paper where the ways in which the outfluxes sample the storage are investigated in detail [*Queloz et al.,* 2015].

4.3. On Reactivity

During our experiment, the largest mass recovery observed was 69%. All tracers thus prove to be reactive in the system, despite the fact that FBAs are often considered conservative tracers and have been used in several hydrological studies specifically for this asset [e.g., *Bowman*, 1984; *Kung et al*., 2000; *Juhler and Mortensen*, 2002]. This experiment was initially not designed for quantifying the tracer mass loss that can be attributed to a specific degradation or removal pathway, nor it aims at identifying the nature of these sinks. Hence, considering the results, we used and interpreted the data at hand and conducted ad hoc testing in order to diagnose the implications of the interactions between hydrological transport and solute reactivity (Appendix B).

Potential passive processes, in particular soil sorption, were regarded using the results of the leaching test (Appendix A) and soil extracts analysis carried out after the end of the experiment. The high FBA recovery of the column leaching tests using the same materials indicates that no sorption occurs in our soil, at least under saturated conditions. In addition, the large number of samples collected at different depths do not contain significant amount of tracer. Note that the method used actually overestimates the concentration of the tracer sorbed, as the soil samples contained residual water at time of collection. These findings are in agreement with previous findings of *Jaynes* [1994] and suggest that active processes—that we simplify here in two categories: ET uptake and microbial degradation—are responsible for the observed mass loss.

Whereas plant uptake was demonstrated for two of the five tracers (as they have been found in the plant's wood and leaves), the measured concentration found would only account for a negligible fraction of the initial mass injected (section B2). It has been shown that these compounds are prone to plant uptake and can be used as a carbon source for plant metabolism [*Bulusu*, 1995; *Bowman et al*., 1997]. The two tracers found in the plant tissues (also in 2014 leaves) are interestingly 2-TFMBA (TR2) and 3-TFMBA (TR5), two trifluoromethylbenzoic acids that were injected only in 2013. TR1, TR3, and TR4 were in contrast all difluorobenzoic acids, and despite a much larger mass of some of them was applied (e.g., TR4, which was additionally reinjected in 2014), there were not observed in the plant extracts. Either the difluorobenzoic acids are not prone to plant uptake, or they are metabolized more readily than trifluoromethylbenzoic acids. However, *Bowman et al*. [1997] reported significant uptake for 2,6-DFBA (TR4) and 3,4-DFBA (TR3). Note that *Salix* spp. are used in phytoremediation to remove chlorobenzoic acids, a by-product of polychlorinated biphenyl [*Susarla et al*., 2002], which also advocates for the ability of willows to uptake these compounds.

As already mentioned (section B3), microbial degradation of FBAs has not been specifically studied, but the similarity between fluoro and chlorobenzoic acids argues for the consideration of microbial degradation as a potential process affecting the tracers in our system. The possible degradation pathway involving dehalogenation in the first place has been assessed by measuring fluoride concentration in the soil water and discharge water. The concentrations are too low to be accountable for a sizable fraction of the FBAs that would have been metabolized by microorganisms, but the negative concentration gradient of fluoride with depth and the brief peak in the discharge observed when the FBAs breakthrough starts speak for a preferential degradation at shallow depth and during a limited period after the tracer injection (i.e., when the tracers is mostly at the top of the column). This is, however, insufficient to understand the global picture of microbial degradation, as a major degradation pathway appears to involve fluorocathechol (not analyzed) as the first breakdown product.

FBAs tracers are thus likely to be affected by ET uptake and microbial activity rather than by soil sorption processes. In this light, the tracer breakthroughs and the temporal distribution of the tracers in the column can be investigated and provide additional information on how the removal mechanisms operate in combination with hydrological transport. As mentioned in section 4.2, the similarity of the tracer outflux dynamics (for the tracer that were significantly recovered) during most of the breakthrough, but a short period following their injection, demonstrates that the differentiation in terms of degradation/removal operates during this limited time at least for TR2, TR4, and TR5. This does not imply that no further mass removal occurs afterward, but in this case these tracers would be equally affected.

TR1 and TR3 do not allow to support the above observations as they have not been detected in the discharge, but looking at their behaviors within the system (Figure 4a) gives some clue about their transport. The pulse of TR1 seems slowly forced downward and remains detectable at every control plane for an extended period (over 2 months). In contrast, TR3 is only detected at 50 cm depth during 2 weeks (14 May–3 June) and is measured in the discharge flow only 8 days after it initially reached the depth of 50 cm. A possible explanation for this discrepancy can be proposed based on the input sequence: the input mass of

TR1 was relatively small, and shortly after its injection subsequent rainfall events occurred, allowing a progressive infiltration and dilution of the pulse in the system. However, the rainfall following injection of TR1 was not sufficient to trigger discharge flow until early May, when the large pulse of TR3 was applied. Therefore, microbial degradation and/or plant uptake may have easily removed the small mass of TR1 during this period. Instead, the mass of TR3 injected in the pulse was much larger and followed by a long dry period in the course of which ET could not have uptake all the mass of tracer in the soil. The observed patterns, plus the fact that TR3 could not be found in the soil analyses, suggest that degradation in the system likely occurred, at least for this tracer.

Having shown experimentally that plant uptake is a possible removal pathway for FBAs, ET fluxes thus provide a major source of non stationarity for solute transport, not only in terms of timing, as it has already been demonstrated, but also in terms of mass export. As an example, let us assume similar *ET* uptake for all tracers and preferential water withdrawal at shallow depth by the willow. The sequence of rainfall that follows an injection would have a great influence on the mass loss and export as it changes solute concentration distribution in the soil profile, thus affecting availability for uptake. It can be noticed in the 2013 injection that the tracers with the highest recovery ratio (TR2 and TR4) were both closely followed by significant rainfall events (Figure 3). These rainfall events were large enough to induce transport of the tracer through the entire profile, as they begin to be detected in the discharge at this occasion. In contrast, TR1 and TR3 inputs were not followed by rainfall and were thus exposed to an extended dry period shortly after their injection. This tracer pulse represents the most accessible water for ET flux, as ET preferentially withdraws shallow water.

TR5 presents an intermediate situation between TR2/4 and TR1/3. The rainfall events that followed the TR5 pulse after 3 days were sufficient to force the tracer pulse down to 50 cm, but it has not been detected deeper in the profile before a large water input occurred on 17 June, also triggering TR5 outflux in the discharge. As it is discussed in the previous section and demonstrated in Figure 6c, the similarity between the breakthroughs of TR5 and TR2/4 suggests that the difference in terms of total recovery of the tracers should originate from the period preceding TR5 breakthrough in the discharge. ET uptake and/or preferential biodegradation at shallow depth could induce this mass removal. Note that microbial degradation can be enhanced by rhizodeposition [*Deavers et al*., 2010; *Vrchotová et al*., 2013] and therefore induced by environmental conditions prompted by the vegetation.

Examining the evolution of soil water tracer concentration during selected dry periods (with no discharge flow and no precipitation) could have informed on where, and at what stage of the tracer transport, degradation processes occur, but the soil water concentrations are subject to important heterogeneity effects preventing interpretation at a fine time scale. In addition, these measurements appear to reflect only part of the picture: all tracers are found in the deepest soil water samples (Figure 4a) much later than their occurrence in the discharge (Figure 3). This could be a consequence of the strong negative pressure applied by the porous cups, which are also able to extract residual pore water tightly bound to the soil matrix. Instead, discharge occurs in high soil moisture conditions and when strong connectivity is prompted. This allows different and more "remote" water pools to contribute to discharge that are able to bypass the volumes sampled the porous cups. The higher soil water concentrations observed for TR2 at 100 cm compared to those at 50 cm support these statements, showing either that the pulse has bypassed the sampling at shallow depth, or that the representability of the samples at either depths due to heterogeneity.

5. Conclusions

The controlled injection of five fluorobenzoate tracers within a vegetated hydrologic control volume subject to erratic rainfall patterns was intended to highlight nonstationarity of the bulk transport processes attributable to variable hydrologic conditions. The results of the 2 year experiment established that the premises on the tracers behavior, known to be conservative and therefore suitable for hydrological studies, were disproved as large differences in mass recovery appeared. This provided nonetheless a valuable data set from our experiments, available as an attachment to this manuscript, as issues on reactivity arose and were addressed in this paper.

The data set serves well the original research question, that is to evaluate how hydrologic fluxes store and sample water and solute within controlled transport volumes, whose interpretation by travel and residence

time distributions is the subject of a companion paper. The experimental results presented are interesting in their own right in that they highlight selective transport properties of a particular class of fluorobenzoate tracers previously thought to be nearly nonreactive but in reality highly sensitive to microbial degradation and plant uptake under the type of unsaturated conditions faced by hydrologic transport.

The experiment shows that the discharge response of tracers pulses is largely nonstationary, not only due to the variation of the climatic forcing, but also due to the prevailing soil moisture and ET deficits during hydrological transport. The results also suggest that moisture conditions are particularly influential during a short period after the pulse injection, as most of the differences in terms of mass loss among the tracers occur during such time. This emphasized the fact that ET uptake and/or microbial degradation potentially operates on specific pools of the water stored that can be different than those used by discharge.

This study suggests previously unknown features of potentially interesting hydrologic tracers suited to distinguishable multiple injections and provides an analysis on the issues to be resolved toward a direct experimental closure of mass balance in hydrologic transport volumes involving significant output fluxes (like in this case ET from a diverse assemblages of vegetation and discharge from a different compliance surface) that are likely to sample stored water and solutes in different ways.

Appendix A: Tracer Validation by Leaching Test

In order to assess the reactivity of the selected chemicals in the soil, a small-scale column experiment has been set up. The column consists of a stainless-steel cylinder with a diameter of 25 cm filled with 50 cm of the same soil mixture used in the lysimeter experiment. A vertical downward flow is induced by maintaining an 1 cm overflow above the soil surface, and can be regulated by changing the pressure head at the outlet. A mixture of the five tracers was added in the inlet zone (overflow) simulating a quasi-instantaneous pulse with a concentration of about 10 mg L^{-1}. Samples were taken every 2 h using a solenoid valve and a fraction collector, and a subset of the collected samples was further analyzed with the same procedure as described in section 2.3.

After 13 days, 94, 100, 97, 100, and 102% of the mass injected was recovered for 2,5-DFBA, 2-TFMBA, 3,4-DFBA, 2,6-DFBA, and 3-TFMBA, respectively. The small mass excess for the last tracer is likely due to measurements error. The breakthrough curves and cumulative mass recovery are presented in Figure S1 in the supporting information. The bimodal shape of the breakthrough curves is likely induced by fluctuations of the discharge rate, which, due to the system setup, could not be maintained perfectly constant during the experiment. These results are in accordance with the finding of *Jaynes* [1994], with a slightly retarded arrival of 3,4-DFBA and 3-TFMBA in regards to the other compounds and mass recovery within a similar range (it is to be noted that we designed the experiment with a residence time about 10 times larger than in *Jaynes* [1994]).

The negligible mass loss and low retardation of the FBAs observed in this experiment for our specific soil, in accordance with the literature [*Bowman*, 1984; *Bowman and Gibbens*, 1992; *Jaynes*, 1994] are justified arguments for the selection of the five FBAs as individual conservative tracers for this study.

Appendix B: Post Hoc Tracer Reactivity Testing

At the end of the experiment, the poor overall recovery of the FBAs indicates that despite they are often considered as nonreactive tracers in the literature, we face potentially diverse processes affecting the amount of unreacted compounds found in the discharge. These processes are either (1) degrading the tracers into by-products within the system, (2) removing the tracers via nonmonitored pathway (i.e., ET flux), and/or (3) accumulating the tracers within the system preventing their release in the discharge water. We investigated the possibility of these pathways a posteriori by measuring tracer accumulation in the plant and in the soil (destructive). Note that plant metabolism and microbial activity may also have transformed parts of the tracers applied by various degradation pathways, leading to a potentially large array of by-products [*Bowman et al*., 1997; *Commandeur and Parsons*, 1990]. A possible microbial degradation pathway involving the release of Fluoride as a by-product was also examined.

B1. Soil Sorption

FBA extraction was performed on raw soil samples (i.e., unsorted of any organic/mineral fraction). Therefore, the levels of FBA can be difficult to interpret, as they can result from soil sorption, but also root uptake or microbial bioaccumulation. We sampled soil cores at different depths and different radial distances from the trunks after the last water flushes, and determine for each sample the content in FBAs and in organic matter (with total organic carbon measurements), so as to analyze possible correlations. A positive correlation of the FBA content with the organic matter would suggest that the FBAs are mainly bound to the organic fraction (roots or microbial mass) rather than sorbed on mineral particles. A vertical gradient of total organic carbon may be expected in our setting based on the root density distribution.

Soil cores were collected with a semicylindrical auger, giving a continuous sample from the surface up to the top of the gravel filter at 2 m depth. Four vertical profiles were collected radially at 0, 15, 30, and 45 cm from the center of the lysimeter, hence at increasing distance from the trunks of the two willows. Each profile was divided into four samples with depth ranging from 0–50, 50–100, 100–150 to 150–200 cm. The samples were dried at 40°C during 24 h, and conditioned in airtight plastic bags. 5–10 g of each sample were used for stirred extraction with 30 mL of MilliQ water during 24 h. The samples were filtered at 0.45 μm with GMF filters (BGB Analytik) and concentrated on a solid phase extraction (SPE) system (Visiprep, Sigma-Aldrich) with 200 mg polymeric reversed-phase cartridges (Oasis HLB 6 cc, Waters) conditioned with 5 mL acetonitrile and 10 mL MilliQ water. After the injection of the 30 mL samples, the FBAs were recovered with 3 mL acetonitrile, concentrated at 0.1 mL and finally diluted at 1 mL with the LC/MS-MS eluent. The quantification was done with LC/MS-MS following the procedure described in section 2.3.

The total organic carbon (TOC) fraction of each sample was determined using the combustion catalytic oxidation method (Shimadzu TOC-V SSM).

No significant trend of carbon content was observed in the "soil" samples, with a mean value of 0.6 and 1.4% for the total organic carbon and inorganic carbon, respectively (see supporting information, Figure S3). The root network is thus considered to be homogeneously distributed in the entire volume of the lysimeter.

Tracer concentration in the soil ranges from 0 to about 10 ng g^{-1}, except for TR3 which has not been detected in any sample (supporting information, Figure S2). Higher tracer content are observed for the deepest samples with the largest distance from the center, reaching about 55 ng g^{-1} for TR5 and up to 260 ng g^{-1} for TR4. Generally, there is a small increase of the concentration (except for TR5) with depth, but no clear trend is observed with the radial distance from the center. The mass measured in the soil represents approximately 0.1, 0.4, 0.9, and 2.3% of the mass injected (on a total unrecovered mass of 100, 33, 99, 40, and 81% at the end of the breakthroughs) for TR1, TR2, TR4, and TR5, respectively. No correlation between the samples' tracer content and the TOC can be noticed, as the low TOC values appear homogeneous in the system, between 0.37% and 0.77%. A TOC content between 0.9% and 1% was observed for the samples corresponding to the center profile at 0–50 cm depth and to the profile at 15 cm from the center at between 100 and 150 cm depth.

B2. Plant Uptake

In order to estimate the FBA content in the biomass, the two willows were cut at the soil surface, and the aerial biomass was divided and weighted as follows: upper twigs, mid twigs, lower twigs, trunk, first-order branches, second and third-order branches. The twigs of each category were further divided into two size-classes (as the age of the twigs may change the amount of tracer that could have been metabolized before sampling). Samples in each category were randomly collected, measured, and weighted. The samples were ground with a helical blade mixer (Ika M20) and a similar filtration and extraction procedure (extraction with water and SPE) as for the soil samples was used. The LC/MS-MS quantification procedure is detailed in section 2.3.

The detection of FBAs in the plant extracts confirms that plant uptake is a viable pathway, in particular with willows. Only TR2 and TR5 were detected, whereas the three other tracers were below the detection limit. TR2 was measured in all samples at a concentration ranging from 165 to 397 ng g^{-1}. The TR2 concentration was significantly lower in the wood samples than in the twigs samples. TR5 concentration were 2 order of magnitude lower than TR2 ranging from 1.6 to 30.6 ng g^{-1}, but also detected in all samples. The

concentrations measured multiplied by the total dry biomass of each sample's category give a crude estimate of the tracer accumulated in the aerial part of the willow, which represent 3.8 mg for TR2 and 0.06 mg for TR5 (0.13% and 0.003% of the TR2/TR5 injected mass, respectively). The fluoride concentrations are presented in the supporting information, Figure S5.

B3. Microbial Degradation

Tracer microbial degradation is difficult to assess, as breakdown pathways are numerous and may differ depending on the microbial communities present in the soil. Specific literature reporting fluorobenzoic acid degradation is relatively poor and limited to mono-fluorobenzoic acids [*Commandeur and Parsons*, 1990; *Motosugi and Soda*, 1983; *Vargas et al*., 2000]. In contrast, degradation of chlorofluorobenzoic acids (CBAs) has been much more investigated (they are by-products of PCBs). Numerous aerobic degradation pathways of CBAs have been described for different bacteria strains. However, similarly to FBAs, most of them usually lead to the production of catechol, which implies the release of a halide ion, or chloro/fluorocatechol [*Commandeur and Parsons*, 1990; *Motosugi and Soda*, 1983; *Patil and Rao*, 2014; *Zaitsev and Karasevich*, 1981]. Fluoride potentially released from microbial degradation would then be washed out, as the soil sorption can only occur by anionic exchange, unlikely in very sandy soil as here. Hence, we analyzed a posteriori a selection of soil water and discharge water samples, in order to identify a possible Fluoride concentration increase due to microbial degradation of FBAs. Fluoride concentration in aqueous samples was determined using ion chromatography (Dionex ICS-3000, USA).

The fluoride concentrations are shown in Figure S5 in supporting information. The fluoride level in the discharge water is generally low, below the analytical limit of calibration (0.10 mg g^{-1}). Two samples show a concentration around 0.20 mg g^{-1} early after the beginning of the first breakthrough in 2013. At the end of the first breakthrough and during the subsequent breakthrough of the 2014 injection, fluoride increases consistently up to 0.15 mg g^{-1}. The soil water samples indicate a low negative gradient with depth.

Acknowledgments

Data are available as supporting information to this paper. The authors would like to thank the Swiss National Science Foundation (SNF) for funding the research project 135241 (Div. I–III). We also acknowledge Dominique Grandjean from the Central Environmental Laboratory (CEL) in EPFL for the chemical analysis and Bernard Sperandio from the Ecohydrology Laboratory (ECHO) in EPFL for the appreciated help during the installation of the lysimeter and sampling phase.

References

Beeson, R. C. (2011), Weighing lysimeter systems for quantifying water use and studies of controlled water stress for crops grown in low bulk density substrates, *Agric. Water Manage.*, *98*(6), 967–976.

Benettin, P., Y. van der Velde, S. E. A. T. M. van der Zee, A. Rinaldo, and G. Botter (2013), Chloride circulation in a lowland catchment and the formulation of transport by travel time distributions, *Water Resour. Res.*, *49*, 4619–4632, doi:10.1002/wrcr.20309.

Benettin, P., A. Rinaldo, and G. Botter (2014), Kinematics of age mixing in advection-dispersion models, *Water Resour. Res.*, *49*, 8539–8551, doi:10.1002/2013WR014708.

Bergström, L. (1990), Use of lysimeters to estimate leaching of pesticides in agricultural soils, *Environ. Pollut.*, *67*, 325–347.

Bertuzzo, E., M. Thomet, G. Botter, and A. Rinaldo (2013), Catchment-scale herbicides transport: Theory and application, *Adv. Water Resour.*, *52*, 232–242.

Beven, K. (2012), *Rainfall-Runoff Modelling: The Primer*, 2nd ed., 457 pp., John Wiley, Chichester, U. K.

Botter, G., E. Bertuzzo, and A. Rinaldo (2010), Transport in the hydrologic response: Travel time distributions, soil moisture dynamics, and the old water paradox, *Water Resour. Res.*, *46*, W03514, doi:10.1029/2009WR008371.

Botter, G., E. Bertuzzo, and A. Rinaldo (2011), Catchment residence and travel time distributions: The master equation, *Geophys. Res. Lett.*, *38*, L11403, doi:10.1029/2011GL047666.

Bowman, R. S. (1984), Evaluation of some new tracers for soil water studies, *Soil Sci. Soc. Am. J.*, *48*(5), 987–993.

Bowman, R. S., and J. F. Gibbens (1992), Difluorobenzoates as nonreactive tracers in soil and ground water, *Ground Water*, *30*(1), 8–14.

Bowman, R. S., J. Schroeder, R. Bulusu, M. Remmenga, and R. Heightman (1997), Plant toxicity and plant uptake of fluorobenzoate and bromide water tracers, *J. Environ. Qual.*, *26*(5), 1292–1299.

Brusseau, M. L., P. S. C. Rao, and R. W. Gillham (1989), Sorption nonideality during organic contaminant transport in porous media, *Crit. Rev. Environ. Control*, *19*(1), 33–99.

Bulusu, R. (1995), *Plant Uptake of Fluorobenzoates Used as Soil and Groundwater Tracers*, N. M. Inst. of Min. and Technol., Socorro, N. M.

Commandeur, L. C. M., and J. R. Parsons (1990), Degradation of halogenated aromatic compounds, *Biodegradation*, *1*(2–3), 207–220.

Dalian, O., and Z. Ronen (2001), Analytical procedure for simultaneous use of seven fluorobenzoates in multitracer tests, *Ground Water*, *39*(3), 366–370.

Deavers, K., T. Macek, U. Karlson, and S. Trapp (2010), Removal of 4-chlorobenzoic acid from spiked hydroponic solution by willow trees (*Salix viminalis*), *Environ. Sci. Pollut. Res.*, *17*(7), 1355–1361.

Divine, C. E., and J. J. McDonnell (2005), The future of applied tracers in hydrogeology, *Hydrogeol. J.*, *13*(1), 255–258.

Flury, M. (1996), Experimental evidence of transport of pesticides through field soils—A review, *J. Environ. Qual.*, *25*(1), 25–45.

Flury, M. (2003), Dyes as tracers for vadose zone hydrology, *Rev. Geophys.*, *41*(1), 1002, doi:10.1029/2001RG000109.

Flury, M., H. Fluehler, W. Jury, and J. Leuenberger (1994), Susceptibility of soil to preferential flow of water—A field study, *Water Resour. Res.*, *30*(7), 1945–1954.

Galdiga, C. U., and T. Greibrokk (1998), Ultra-trace determination of fluorinated aromatic carboxylic acids in aqueous reservoir fluids using solid-phase extraction in combination with gas chromatography-mass spectrometry, *J. Chromatogr. A*, *793*(2), 297–306.

Guidi, W., E. Piccioni, and E. Bonari (2008), Evapotranspiration and crop coefficient of poplar and willow short-rotation coppice used as vegetation filter, *Bioresour. Technol.*, *99*(11), 4832–4840.

Harman, C. (2015), Time-variable transit time distributions and transport: Theory and application to storage-dependent transport of chloride in a watershed, *Water Resour. Res.*, *50*, 1–30, doi:10.1002/2014WR015707.
Harman, C. J., P. S. C. Rao, N. B. Basu, G. S. McGrath, P. Kumar, and M. Sivapalan (2011), Climate, soil, and vegetation controls on the temporal variability of vadose zone transport, *Water Resour. Res.*, *47*, W00J13, doi:10.1029/2010WR010194.
Hrachowitz, M., C. Soulsby, D. Tetzlaff, I. A. Malcolm, and G. Schoups (2010a), Gamma distribution models for transit time estimation in catchments: Physical interpretation of parameters and implications for time-variant transit time assessment, *Water Resour. Res.*, *46*, W10536, doi:10.1029/2010WR009148.
Hrachowitz, M., C. Soulsby, D. Tetzlaff, and M. Speed (2010b), Catchment transit times and landscape controls—Does scale matter?, *Hydrol. Processes*, *24*(1), 117–125.
Hrachowitz, M., H. Savenije, T. A. Bogaard, D. Tetzlaff, and C. Soulsby (2013), What can flux tracking teach us about water age distribution patterns and their temporal dynamics?, *Hydrol. Earth Syst. Sci.*, *17*(2), 533–564.
Jaynes, D. B. (1994), Evaluation of fluorobenzoate tracers in surface soils, *Ground Water*, *32*(4), 532–538.
Juhler, R. K., and A. P. Mortensen (2002), Analysing fluorobenzoate tracers in groundwater samples using liquid chromatography-tandem mass spectrometry: A tool for leaching studies and hydrology, *J. Chromatogr. A*, *957*(1), 11–16.
Käss, W. (1998), *Tracing Techniques in Geohydrology*, 581 pp., A. A. Balkema, Rotterdam, Netherlands.
Kendall, C., and E. A. Caldwell (1998), *Fundamentals of Isotope Geochemistry*, 870 pp., Elsevier, Amsterdam, Netherlands.
Kirchner, J., D. Tetzlaff, and C. Soulsby (2010), Comparing chloride and water isotopes as hydrological tracers in two Scottish catchments, *Hydrol. Processes*, *24*(12), 1631–1645.
Kung, K.-J. S., E. J. Kladivko, T. J. Gish, T. S. Steenhuis, G. Bubenzer, and C. S. Helling (2000), Quantifying preferential flow by breakthrough of sequentially applied tracers silt loam soil, *Soil Sci. Soc. Am. J.*, *64*(4), 1296–1304.
Lasa, J., and I. Åšliwka (1990), Application of gas chromatography with electron-capture detection to trace analysis of halogenated compounds, *J. Chromatogr. A*, *509*(1), 115–121.
Lindstrom, G., and A. Rodhe (1986), Modeling water exchange and transit times in till basins using oxygen-18, *Nord. Hydrol.*, *17*(4–5), 325–334.
Maloszewski, P., W. Rauert, P. Trimborn, A. Herrmann, and R. Rau (1992), Isotope hydrological study of mean transit times in an alpine basin (Wimbachtal, Germany), *J. Hydrol.*, *140*(1–4), 343–360.
McCarthy, J. F., K. M. Howard, and L. D. McKay (2000), Effect of pH on sorption and transport of fluorobenzoic acid ground water tracers, *J. Environ. Qual.*, *29*(6), 1806–1813.
McDonnell, J. J., and K. Beven (2014), Debates—The future of hydrological sciences: A (common) path forward? A call to action aimed at understanding velocities, celerities and residence time distributions of the headwater hydrograph, *Water Resour. Res.*, *50*, 5342–5350, doi:10.1002/2013WR015141.
McDonnell, J. J., et al. (2010), How old is streamwater? Open questions in catchment transit time conceptualization, modelling and analysis, *Hydrol. Processes*, *24*(12), 1745–1754.
McGuire, K. J., and J. J. McDonnell (2006), A review and evaluation of catchment transit time modeling, *J. Hydrol.*, *330*(3–4), 543–563.
McGuire, K. J., M. Weiler, and J. J. McDonnell (2007), Integrating tracer experiments with modeling to assess runoff processes and water transit times, *Adv. Water Resour.*, *30*(4), 824–837.
Misiak, K., E. Casey, and C. D. Murphy (2011), Factors influencing 4-fluorobenzoate degradation in biofilm cultures of *Pseudomonas knackmussii* B13, *Water Res.*, *45*(11), 3512–3520.
Mortensen, A. P., K. H. Jensen, B. Nilsson, and R. K. Juhler (2004), Multiple tracing experiments in unsaturated fractured clayey till, *Vadose Zone J.*, *3*(2), 634–644.
Motosugi, K., and K. Soda (1983), Microbial degradation of synthetic organochlorine compounds, *Experientia*, *39*(11), 1214–1220.
Niemi, A. J. (1977), Residence time distributions of variable flow processes, *Int. J. Appl. Radiat. Isot.*, *28*(10–11), 855–860.
Patil, Y., and P. Rao (2014), *Applied Bioremediation—Active and Passive Approaches*, Intech Open Sci. Online Publ., Rijeka, Croatia.
Persson, G. (1995), Willow stand evapotranspiration simulated for Swedish soils, *Agric. Water Manage.*, *28*(4), 271–293.
Queloz, P., L. Carraro, P. Benettin, G. Botter, A. Rinaldo, and E. Bertuzzo (2015), Transport of fluorobenzoate tracers in a vegetated hydrologic control volume: 2. Theoretical inferences and modeling, *Water Resour. Res.*, *51*, doi:10.1002/2014WR016508.
Rinaldo, A., and A. Marani (1987), Basin scale model of solute transport, *Water Resour. Res.*, *23*(11), 2107–2118.
Rinaldo, A., A. Marani, and A. Bellin (1989), On mass response functions, *Water Resour. Res.*, *25*(7), 1603–1617.
Rinaldo, A., K. J. Beven, E. Bertuzzo, L. Nicotina, J. Davies, A. Fiori, D. Russo, and G. Botter (2011), Catchment travel time distributions and water flow in soils, *Water Resour. Res.*, *47*, W07537, doi:10.1029/2011WR010478.
Rodhe, A., L. Nyberg, and K. Bishop (1996), Transit times for water in a small till catchment from a step shift in the oxygen 18 content of the water input, *Water Resour. Res.*, *32*(12), 3497–3511.
Rodriguez-Iturbe, I., A. Porporato, L. Ridolfi, V. Isham, and D. R. Coxi (1999), Probabilistic modelling of water balance at a point: The role of climate, soil and vegetation, *Proc. R. Soc. London, Ser. A*, *455*(1990), 3789–3805.
Roth, K., W. A. Jury, H. Fluhler, and W. Attinger (1991), Transport of chloride through an unsaturated field soil, *Water Resour. Res.*, *27*(10), 2533–2541.
Schaeffer, S., D. Williams, and D. Goodrich (2000), Transpiration of cottonwood/willow forest estimated from sap flux, *Agric. For. Meteorol.*, *105*(1–3), 257–270.
Schoen, R., J. P. Gaudet, and T. Bariac (1999), Preferential flow and solute transport in a large lysimeter, under controlled boundary conditions, *J. Hydrol.*, *215*(1–4), 70–81.
Serres-Piole, C., A. Commarieu, H. Garraud, R. Lobinski, and H. Preud'homme (2011), New passive water tracers for oil field applications, *Energy Fuels*, *25*(10), 4488–4496.
Simic, E., and G. Destouni (1999), Water and solute residence times in a catchment: Stochastic-mechanistic model interpretation of ^{18}O transport, *Water Resour. Res.*, *35*(7), 2109–2119.
Stetzenbach, K. J., S. L. Jensen, and G. M. Thompson (1982), Trace enrichment of fluorinated organic acids used as ground-water tracers by liquid chromatography, *Environ. Sci. Technol.*, *16*(5), 250–254.
Stewart, M. K., and J. J. McDonnell (1991), Modeling base flow soil water residence times from deuterium concentrations, *Water Resour. Res.*, *27*(10), 2681–2693.
Susarla, S., V. F. Medina, and S. C. McCutcheon (2002), Phytoremediation: An ecological solution to organic chemical contamination, *Ecol. Eng.*, *18*(5), 647–658.
van der Velde, Y., P. J. J. F. Torfs, S. E. A. T. M. van der Zee, and R. Uijlenhoet (2012), Quantifying catchment-scale mixing and its effect on time-varying travel time distributions, *Water Resour. Res.*, *48*, W06536, doi:10.1029/2011WR011310.

Vargas, C., B. Song, M. Camps, and M. M. Häggblom (2000), Anaerobic degradation of fluorinated aromatic compounds, *Appl. Microbiol. Biotechnol.*, *53*(3), 342–347.

Vrchotová, B., P. Lovecká, M. Drazková, M. Macková, and T. Macek (2013), Influence of root exudates on the bacterial degradation of chlorobenzoic acids, *Sci. World J.*, *0132*, 8.

Wolock, D. M., J. Fan, and G. B. Lawrence (1997), Effects of basin size on low-flow stream chemistry and subsurface contact time in the Neversink River watershed, New York, *Hydrol. Processes*, *11*(9), 1273–1286.

Zaitsev, G. M., and I. Karasevich (1981), Utilization of 4-chlorobenzoic acid by arthrobacter globiformis, *Mikrobiologiia*, *50*(1), 35–40.